



저작자표시-비영리-변경금지 2.0 대한민국

이용자는 아래의 조건을 따르는 경우에 한하여 자유롭게

- 이 저작물을 복제, 배포, 전송, 전시, 공연 및 방송할 수 있습니다.

다음과 같은 조건을 따라야 합니다:



저작자표시. 귀하는 원저작자를 표시하여야 합니다.



비영리. 귀하는 이 저작물을 영리 목적으로 이용할 수 없습니다.



변경금지. 귀하는 이 저작물을 개작, 변형 또는 가공할 수 없습니다.

- 귀하는, 이 저작물의 재이용이나 배포의 경우, 이 저작물에 적용된 이용허락조건을 명확하게 나타내어야 합니다.
- 저작권자로부터 별도의 허가를 받으면 이러한 조건들은 적용되지 않습니다.

저작권법에 따른 이용자의 권리는 위의 내용에 의하여 영향을 받지 않습니다.

이것은 [이용허락규약\(Legal Code\)](#)을 이해하기 쉽게 요약한 것입니다.

[Disclaimer](#)

이학석사학위논문

**Room Temperature Ferromagnetism with  
Large Magnetic Moment at Low Field in  
Rare-Earth-doped BiFeO<sub>3</sub> Thin Films**

**상온의 낮은 자기장에서 높은 자기 모멘트를  
보이는 희토류가 첨가된 비스무스  
철산화물의 강자성**

2013년 2월

서울대학교 대학원  
물리천문학부  
김 태 영



**Room Temperature Ferromagnetism with  
Large Magnetic Moment at Low Field in Rare-  
Earth-doped BiFeO<sub>3</sub> Thin Films**

**상온의 낮은 자기장에서 높은 자기 모멘트를  
보이는 희토류가 첨가된 비스무스  
철산화물의 강자성**

지도교수 Nguyen Hoa Hong  
이 논문을 이학석사학위논문으로 제출함

2012년 12월

서울대학교 대학원  
물리천문학부  
김 태 영

김태영의 석사학위논문을 인준함  
2012년 12월

위원장	<hr/>	박 제 근	(인)
부위원장	<hr/>	Nguyen Hoa Hong	(인)
위원	<hr/>	박 철 환	(인)

## ABSTRACT

### **Room Temperature Ferromagnetism with Large Magnetic Moment at Low Field in Rare-Earth-doped BiFeO<sub>3</sub> Thin Films**

Tae-Young Kim

Dept. of Physics and Astronomy

Graduate School

Seoul National University

BiFeO<sub>3</sub> is a promising multiferroic material due to its high ferroelectric (1103 K) and antiferromagnetic (643 K) ordering temperatures. Previous reports have suggested that by reducing the dimensionality, the spiral magnetic ordering could be suppressed; therefore, the magnetic properties could be modified. In BiFeO<sub>3</sub>, if Bi is partially substituted by a small amount of divalent or trivalent metal ions, or Fe is substituted by transition metal ion, a significant enhancement in magnetization can be achieved. Thin films of Rare Earth (Re) - doped BiFeO<sub>3</sub> (where RE = Sm, Ho, Pr and Nd) were grown on LaAlO<sub>3</sub> substrates by using pulsed laser deposition technique. All the films show a single phase of rhombohedral structure with space group *R3c*. The saturated magnetization in the Ho- and Sm- doped films is much larger than those reported in literature, and was observed at a quite low field as of 0.2 T. In the case of Ho and Sm doping, the magnetization increases when the film becomes thinner, suggesting that the observed magnetism is mostly due to surface

effect. In the case of Nd doping, even though the thin film has large magnetic moment, the mechanism seems to be different.

**Keywords: BFO, Rare-Earth, Ferromagnetism, Thin films**

**Student ID Number: 2011-20396**

## **Contents**

<b>ABSTRACT.....</b>	<b>I</b>
<b>List of Figures.....</b>	<b>V</b>
<b>List of Tables.....</b>	<b>VII</b>
<b>Chapter 1: Introduction.....</b>	<b>1</b>
<b>1.1. Multiferroic materials; Bismuth Ferrite Oxides (BFO).....</b>	<b>1</b>
<b>1.2. Ferromagnetic enhancement in BiFeO<sub>3</sub> thin films:</b>	
<b>Dimension and Doping .....</b>	<b>3</b>
<b>Chapter 2: Experimental Methods.....</b>	<b>4</b>
<b>2.1. Sample Preparation.....</b>	<b>4</b>
<b>2.1.1. Sol-gel auto ignition Method.....</b>	<b>5</b>
<b>2.1.2. Pulsed Laser Deposition (PLD).....</b>	<b>5</b>
<b>2.2. Measurements.....</b>	<b>7</b>
<b>2.2.1. X-Ray Diffraction (XRD).....</b>	<b>7</b>
<b>2.2.2. Superconducting Quantum Interference Device</b>	
<b>(SQUID) .....</b>	<b>8</b>
<b>2.2.3. X-Ray Photoelectron Spectroscopy (XPS) .....</b>	<b>9</b>
<b>Chapter 3: Results and Discussions.....</b>	<b>10</b>
<b>3.1. Structural Properties.....</b>	<b>10</b>
<b>3.2. Magnetic Properties.....</b>	<b>13</b>
<b>3.2.1. Sm- and Ho- doped BFO thin films.....</b>	<b>13</b>
<b>3.2.2. RE- doped BFO thin films .....</b>	<b>17</b>
<b>3.3. BFO Films' Chemical States.....</b>	<b>20</b>

<b>Chapter 4: Conclusions.....</b>	<b>22</b>
<b>Appendix.....</b>	<b>23</b>
<b>References.....</b>	<b>25</b>
<b>국문초록 (Abstract in Korean).....</b>	<b>26</b>



## List of Figures

<b>Fig. 1:</b> Magnetic hysteresis loops measured by vibrating sample magnetometry for a 70-nm-thick BFO film. Inset (a) thickness dependence of saturated magnetization and inset (b) preliminary ME measurement [2].....	3
<b>Fig. 2:</b> Magnetic moment versus magnetic field of Dy- doped BFO nanoparticles at room temperature [5].....	3
<b>Fig. 3:</b> The schematic diagram of PLD Technique [13].....	6
<b>Fig. 4:</b> Schematic of 4-circle diffractometer [14].....	7
<b>Fig. 5:</b> Highly sensitive magnetometers: SQUID [15].....	8
<b>Fig. 6:</b> Schematic diagram for the XPS Emission Process [16].....	9
<b>Fig. 7:</b> XRD diffraction patterns for 200 nm-thick-RE <sub>0.1</sub> Bi <sub>0.9</sub> FeO <sub>3</sub> films (where RE= Sm, Ho, Pr and Nd) grown on LaAlO <sub>3</sub> substrates.....	12
<b>Fig. 8:</b> XRD diffraction patterns for Nd-doped BiFeO <sub>3</sub> films with different Nd concentration (as of 5 and 10%), and different thickness (as of 10 and 200 nm) grown on LaAlO <sub>3</sub> substrates.....	12
<b>Fig. 9:</b> Magnetization versus magnetic field taken at 300 K for 200 nm-thick Sm <sub>0.1</sub> Bi <sub>0.9</sub> FeO <sub>3</sub> and Ho <sub>0.1</sub> Bi <sub>0.9</sub> FeO <sub>3</sub> films.....	13
<b>Fig. 10:</b> Magnetization versus magnetic field taken at 300 K for 200 nm-thick Ho <sub>0.05</sub> Bi <sub>0.95</sub> FeO <sub>3</sub> and Ho <sub>0.1</sub> Bi <sub>0.9</sub> FeO <sub>3</sub> films.....	14
<b>Fig. 11:</b> Magnetization versus magnetic field taken at 300 K for Ho <sub>0.1</sub> Bi <sub>0.9</sub> FeO <sub>3</sub> films with thickness of 10 and 200nm. The inset shows the zoom for low field region of <i>M-H</i> of the 200 nm-thick-film.....	16
<b>Fig. 12:</b> Magnetization versus magnetic field taken at 300 K for 200 nm-thick Re <sub>0.1</sub> Bi <sub>0.9</sub> FeO <sub>3</sub> films (where Re= Sm, Ho, Pr and Nd). The inset show the <i>M-H</i> curves of undoped BiFeO <sub>3</sub> films with similar thickness for comparison.....	17

**Fig. 13:** Magnetization versus magnetic field taken at 300 K for 10 nm-thick  $\text{Re}_{0.1}\text{Bi}_{0.9}\text{FeO}_3$  films (where RE= Sm, Ho, Pr and Nd). The inset show the  $M$ - $H$  curves of undoped  $\text{BiFeO}_3$  films with similar thickness for comparison.....**18**

**Fig. 14:** XPS spectra of the Fe ions for the 200 nm-thick  $\text{Re}_{0.1}\text{Bi}_{0.9}\text{FeO}_3$  films (where RE= Sm, Ho, Pr and Nd).....**21**

# List of Tables

**Table. 1:** PLD conditions for making RE- doped BFO thin films.....6

## **Chapter 1: Introduction**

### **1.1. Multiferroic materials; Bismuth Ferrite Oxides (BFO)**

$\text{BiFeO}_3$  (BFO) is one of promising multiferroic materials due to its high ferroelectric (about 1100 K) and antiferromagnetic (about 650 K) ordering temperatures, that are much higher than room temperature.  $\text{BiFeO}_3$  exhibits G-type antiferromagnetism due to the local spin ordering of  $\text{Fe}^{3+}$  which forms a cycloidal spiral spin structure having spin periodicity of 62 nm. There are ways to suppress the spiral magnetic ordering by applying a very high magnetic field, or reducing the dimensions of the sample, or by chemical substitution of  $\text{Bi}^{3+}$  or  $\text{Fe}^{3+}$  by other ions of comparable ionic sizes [1].

There are many multiferroic materials, which have the simultaneous ferroelectricity, ferromagnetism and ferroelasticity. So, these multiferroic materials can be used in future electronic devices, such as information storage, sensors, etc. Among these multiferroic materials, BFO has been an especially interesting one, because different from other materials, it shows the multiferroic properties at room temperature.

## **1.2. Ferromagnetic enhancement in BiFeO<sub>3</sub> thin film; Dimension and Doping**

Reduction in dimension is shown to enhance the magnetization in thin films and in nanoparticles [2, 3]. There are many reports on the enhancement of magnetization of BiFeO<sub>3</sub> in the bulk, thin films, and nanoparticles, on the Bi-site substitution by selected trivalent rare-earth and divalent ions, or on the Fe-site substitution by transition metal ions. Liu et al. suggested that the probable reason for higher magnetization after substitution of Eu<sup>3+</sup> is a presence of the Rare-Earth-(RE) orthoferrite impurity phase [4]. On the other hand, in certain cases, as reported by Qian et al. for Dy<sup>3+</sup> substitution, there is a large decrease in the particle size after substitution, and this could be the reason for an increased magnetization after substitution [5]. Recently, Thakuria and Joy showed that the magnetic moment of the nanoparticles could be enhanced 3 times by substituting Bi by Ho. However, the reported saturated magnetization is still found only at a quite high field as of 6 T [1].

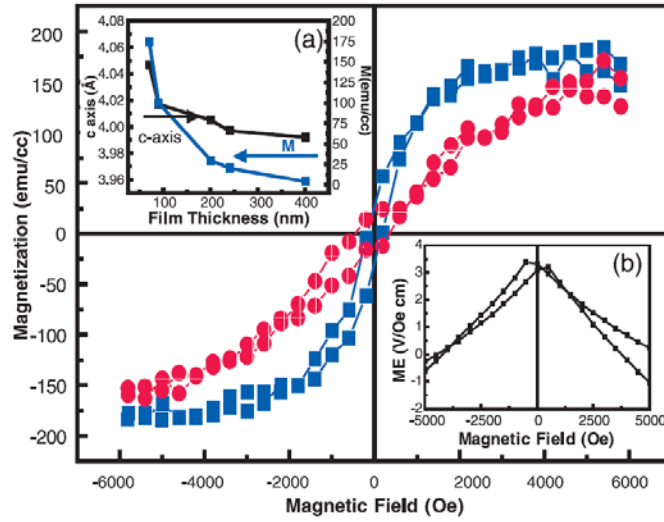


Fig. 1: Magnetic hysteresis loops measured by vibrating sample magnetometry for a 70 nm-thick-BiFeO<sub>3</sub> film. Inset (a) thickness dependence of saturated magnetization and inset (b) preliminary ME measurement [2]

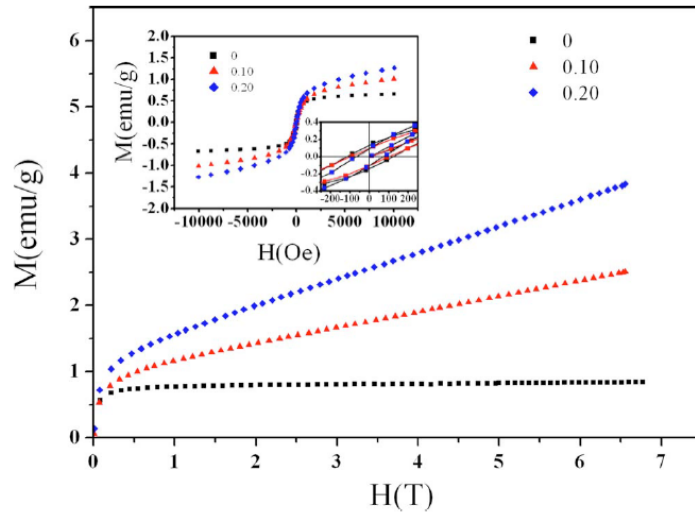


Fig. 2: Magnetic moment versus magnetic field of Dy- doped BFO nanoparticles at room temperature [5]

## **Chapter 2: Experimental Methods**

### **2.1. Sample Preparation**

We made  $RE_xBi_{1-x}FeO_3$  ceramic targets (where RE= Sm, Ho, Pr and Nd;  $x = 0, 0.05$  and  $0.1$ ) by a sol-gel auto ignition method. Rare- Earth- (RE)-doped  $BiFeO_3$  (RBFO) thin films have been fabricated by Pulsed Laser Deposition (PLD) technique (excimer KrF laser with  $\lambda = 248$  nm; the repetition rate was 13 Hz and the energy density was  $2.1$  J/cm<sup>2</sup>), with typical thicknesses of 10 and 200 nm. All the films were grown on (001)  $LaAlO_3$  (LAO) substrates. During deposition, the substrate temperature was kept at  $700$  °C and the oxygen partial pressure ( $P_{O_2}$ ) was  $1.4 \times 10^{-3}$  Torr. After deposition, the sample was kept in the chamber at  $500$  °C with the same oxygen partial pressure as during deposition for 30 min, and then finally cooled down slowly to room temperature.

### 2.1.1. Sol-gel auto ignition Method

We used sol-gel auto ignition method to fabricate BFO nanopowders. First, we put required chemicals (BFO and RE elements) and citric acid in a beaker. And we whirled and heated it using the hot plate and magnetic bar. The temperature was 100 to 300 °C, and the rotating speed was 500 ~ 600 mph. Then we grinded it in a mortar until it becomes fine. And, using by mold and hand manual press, we made the pellet from the powders. After making pellets, we annealed them in a box furnace twice; 500 °C and 900 °C for 10 hrs separately.

### 2.1.2 Pulsed Laser Deposition (PLD)

Pulsed Laser Deposition (PLD) is one of the significant tools in order to fabricate thin films both for scientific research and commercial application. The process is as in the following. First we fix the ceramic target in a chamber. Second, we use the laser beam to shot the target, and then a plasma plume goes to a substrate which is heated to a high temperature. When fabricating a sample, the chamber is maintained in a ultra-high vacuum.



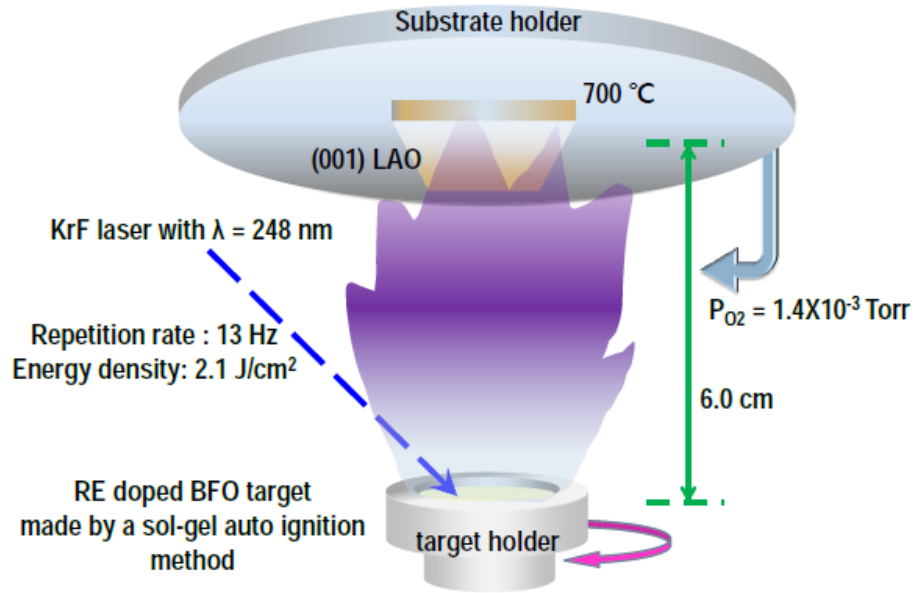


Fig. 3: The schematic diagram of PLD Technique [13]

PLD conditions	
Type	KrF Excimer Laser (248 nm)
Target	RE <sub>x</sub> Bi <sub>1-x</sub> FeO <sub>3</sub> ceramic target ( RE = Sm, Ho, Pr and Nd; x=0, 0.05, 0.01)
Substrate	LaAlO <sub>3</sub> (5x5x0.5 mm <sup>2</sup> )
Substrate Temperature	700 °C
Oxygen Partial Pressure	1.4x10 <sup>-3</sup> Torr
Repetition Rate	13 Hz
Energy density	2.1 J/cm <sup>2</sup>

Table. 1: PLD conditions for making RE- doped BFO thin films

## 2.2. Measurements

### 2.2.1. X-Ray Diffraction (XRD)

X-Ray Diffraction (XRD) measurement is one of the most important tools to see the structure of materials; bulk and thin films, etc. This machine radiates X-ray to the material and detects the reflected beams. So, it is nondestructive and can be used to any materials including metal, alloys, powders and thin films. By the Bragg's law,

$$n\lambda = 2d\sin \theta$$

we can analyze the crystallinity and lattice parameters.

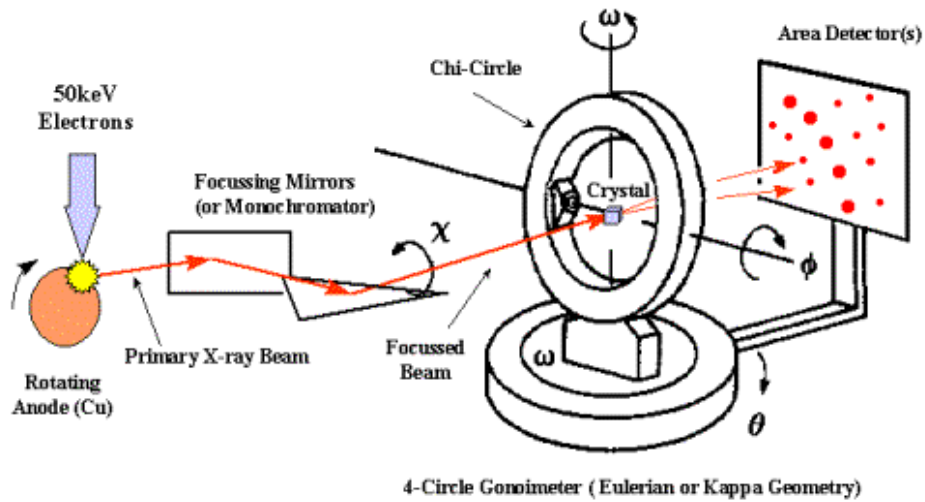


Fig. 4: Schematic of 4-circle diffractometer [14]

### 2.2.2. Superconducting Quantum Interference Device (SQUID)

Superconducting Quantum Interference Device (SQUID) is the tool to measure the magnetization of some samples. This tool uses a superconducting loop; inside this loop a Josephson junction is placed. SQUID can measure many forms of samples such as bulk, powder and thin films. So, this is useful to many fields including physics, chemistry, material science and electrical engineering. Actually, we used the MPMS SQUID of Quantum Design.

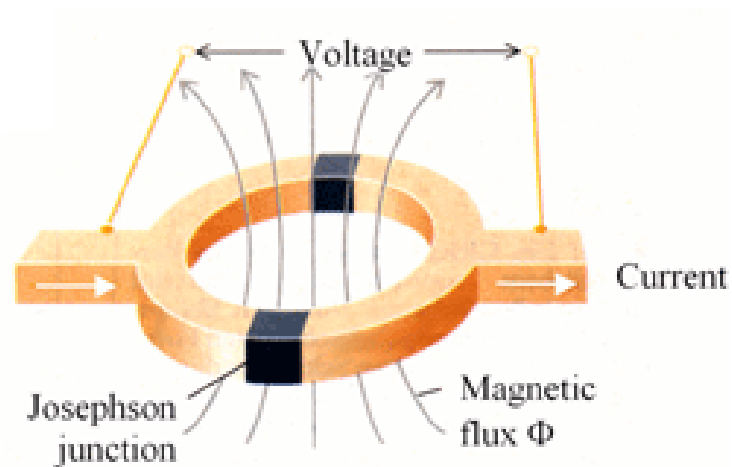


Fig. 5: Highly sensitive magnetometers: SQUID [15]

### 2.2.3. X-Ray Photoelectron Spectroscopy (XPS)

X-ray Photoelectron Spectroscopy (XPS) is a good measurement tool to investigate the surface state of samples, chemical composition and the electron's states. Also this tool is known as Electron Spectroscopy for Chemical Analysis (ESCA). X-ray attacks a sample and then a photoelectron comes out. So, by calculating the energy of this photoelectron, we can know the binding energy of an electron. Especially, we can see the chemical shift of peaks. Therefore, we can get to understand if there is any change with sample's state such as oxidation, valency, etc.

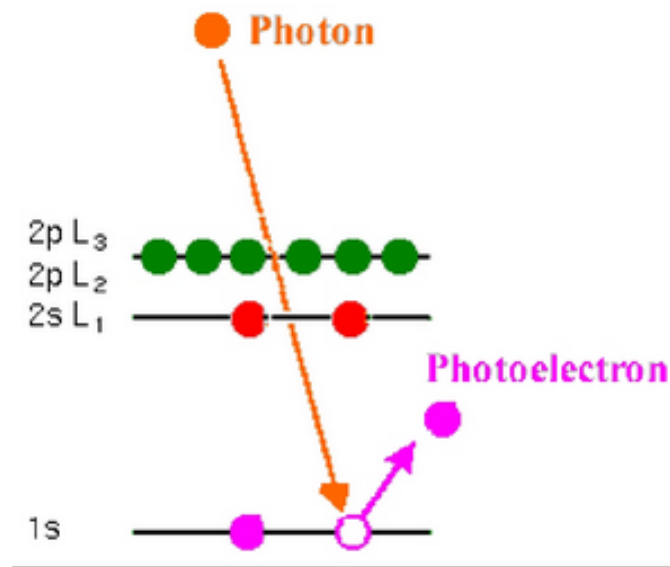


Fig. 6: Schematic diagram for the XPS Emission Process [16]

## Chapter 3: Results and Discussions

We used High Resolution (HR) XRD to analyze the structural properties of thin films. Magnetic properties were investigated by measuring the magnetic moment using a SQUID system. The surface chemical state of thin films was studied by using XPS measurement.

### 3.1. Structural Properties

The XRD diffraction patterns of RE-BFO are shown in Fig. 7 gives a comparison for all the doping cases (for 10% of doping concentration, and thickness of 200 nm). As one can see, there is no drastic change in structure depending on the type of RE elements. All the films show a rhombohedral structure with very sharp peaks of BFO phase. No peak of alien phase appears in the spectra, and the crystallinity is good. Doping of different RE elements with the same concentration only causes some shift in the position of the peaks, indicating some change in lattice parameters. The out-of-plane parameter was determined as of 3.925, 3.925, 3.9329 and 3.922 Å for Sm, Ho, Nd and Pr doping cases, respectively. It seems that the structure is distorted the most in the Pr doping case, and this is in accord with the fact that the ionic radii of  $\text{Pr}^{3+}$  is also quite large (as of 1.266 Å) in comparison to those of the original  $\text{Bi}^{3+}$  (as of 1.17 Å);  $\text{Ho}^{3+}$  (0.901 Å), and  $\text{Nd}^{3+}$  (as of 1.08 Å). [6] From Fig. 8, one can see that changing concentration of doping, or changing the film thickness does not change the structure of the RE- doped BFO films. The BFO films doped with 5 or 10% of Nd with thickness of 200 nm have the same structure,

and the 10 nm- and 200 nm-thick-BFO doped with Nd for the same concentration as of 10% have similar structure as well. Only we note that the crystallinity seems to get a bit worse in the very thin film case, and the lattice parameters are modified (out-of-plane lattice parameters of Nd- and Pr- doped BFO have become 3.932 and 3.937 Å, respectively). In 2007, as for BFO films grown on LaAlO<sub>3</sub> substrates, Rana et al. observed a drastic change from rhombohedral to tetragonal phase when the thickness decreases [7]. However this structural change is not observed in our RE-doped BFO films.

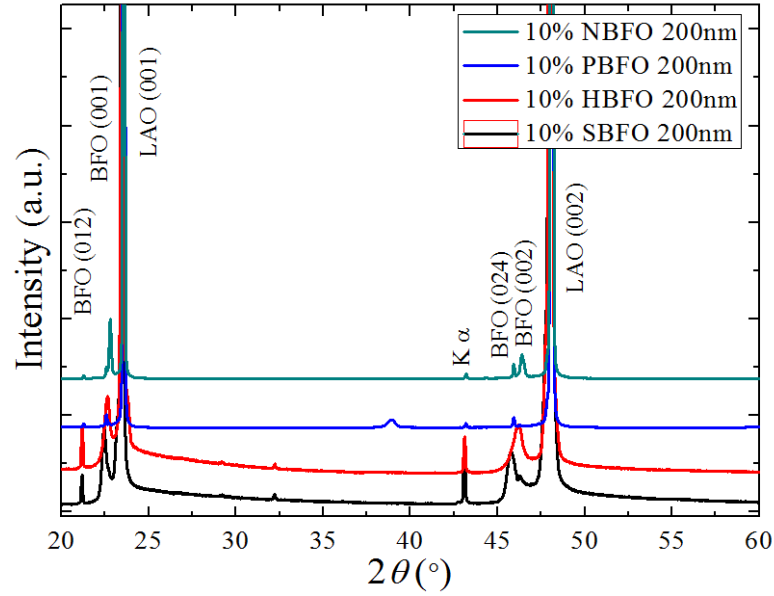


Fig. 7: XRD diffraction patterns for 200 nm-thick- $\text{RE}_{0.1}\text{Bi}_{0.9}\text{FeO}_3$  films (where RE= Sm, Ho, Pr and Nd) grown on  $\text{LaAlO}_3$  substrates

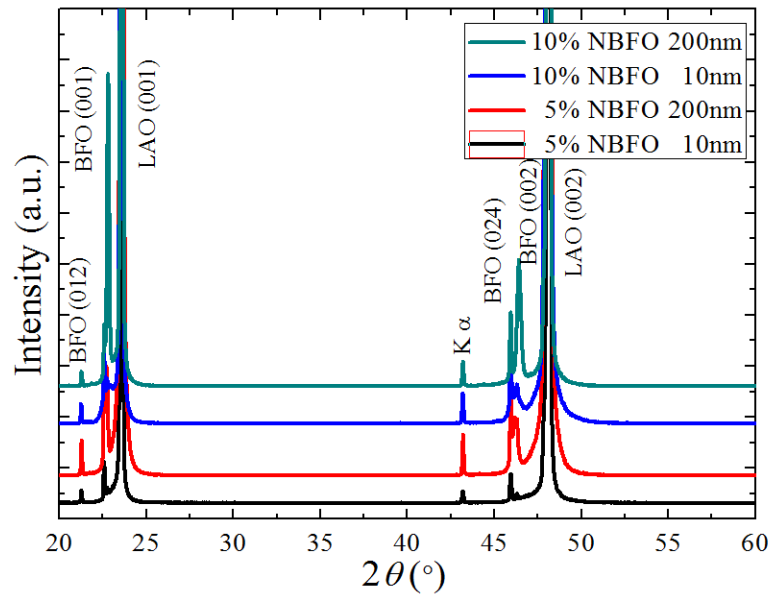


Fig. 8: XRD diffraction patterns for Nd-doped  $\text{BiFeO}_3$  films with different Nd concentration (as of 5 and 10%), and different thickness (as of 10 and 200 nm) grown on  $\text{LaAlO}_3$  substrates

## 3.2. Magnetic Properties

### 3.2.1. Sm- and Ho- doped BFO thin films

Magnetization versus magnetic field taken at 300 K for Sm- and Ho- doped BFO films is shown in Fig. 9. From Fig. 9, one can see that with the same concentration of doping as 10%, with a thickness of 200 nm (not very thin), both films of Sm- doped and Ho- doped BFO films show quite strong ferromagnetic ordering. Even though the magnetic moment of Ho doping case is slightly larger than that of Sm case ( $11 \text{ emu/cm}^3$  for the former and  $7 \text{ emu/cm}^3$  for the latter), we can take these two as roughly the same.

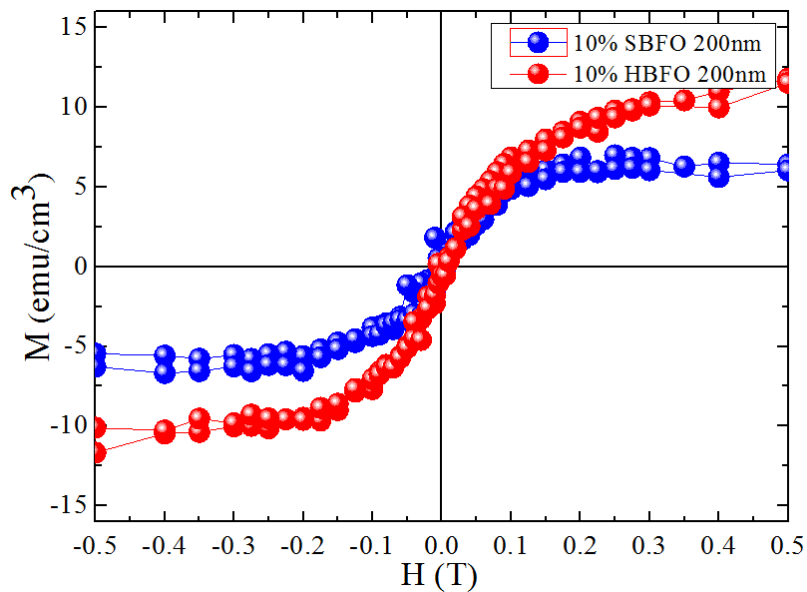


Fig. 9: Magnetization versus magnetic field taken at 300 K for 200 nm-thick  $\text{Sm}_{0.1}\text{Bi}_{0.9}\text{FeO}_3$  and  $\text{Ho}_{0.1}\text{Bi}_{0.9}\text{FeO}_3$  films



Seeing from another aspect, in order to verify whether the doping concentration may influence the magnetic moment of the films or not, one can see the difference shown in Fig. 10 for the typical Ho doping case. It is found that the 10% doping case may give magnetic moment of 2 times larger than that of the 5% doping case. Another point needed to look at is the thickness dependence of the magnetization.

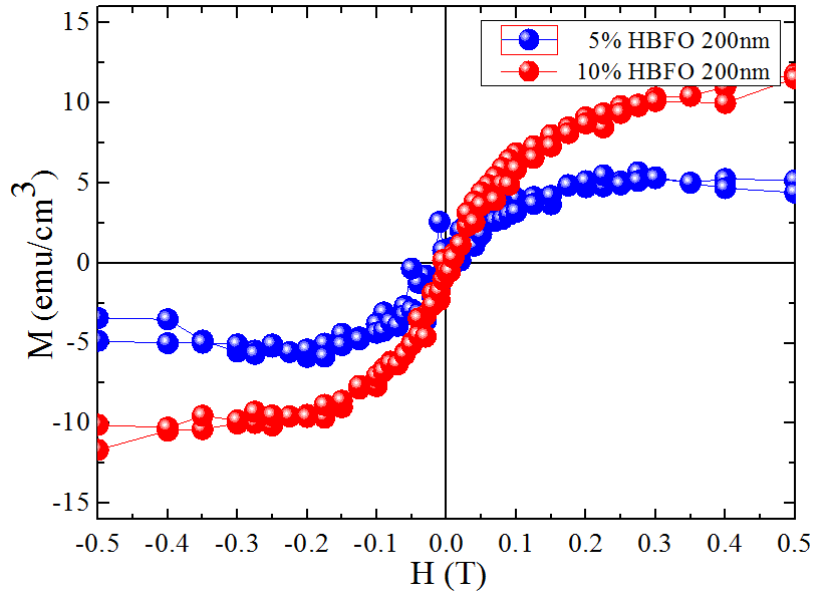


Fig. 10: Magnetization versus magnetic field taken at 300 K for 200 nm-thick  $\text{Ho}_{0.05}\text{Bi}_{0.95}\text{FeO}_3$  and  $\text{Ho}_{0.1}\text{Bi}_{0.9}\text{FeO}_3$  films

Fig. 11 shows that the saturated magnetization ( $M_s$ ) can rise up to about 120  $\text{emu}/\text{cm}^3$  for the 10 nm-thick- Ho- doped BFO film (equivalent to about  $0.8 \mu_B/\text{f.u.}$ ), in comparison to the magnitude of 7  $\text{emu}/\text{cm}^3$  for the 200 nm-thick- one. It is seen that doping Ho (and Sm, also very similarly) partially for Bi in BFO films can make BFO to become room temperature ferromagnetic with a quite large magnetic

moment. Our undoped BFO films fabricated with the same conditions could be ferromagnetic, but the ferromagnetism is quite weak (about 2 orders smaller) (see the insets of Fig 12 and 13, and Ref. 8). Some other group also got ferromagnetic ordering in Ho-doped BFO, however with much smaller magnitude, and the  $M_s$  was obtained at much larger field (as of 6 T), while we got much a larger  $M_s$  but at much lower field (as of 0.2 T). This is quite meaningful for applications. One thing we need to note about the Sm and Ho doping cases is that the magnetism in this case seems to have surface/interface nature. Looking closely and carefully at the raw magnetic data (after subtracting substrate's data) of Ho and Sm cases, we have found that the saturated magnetic moments of the 10 nm-thick film and the 200 nm-thick film have almost the same value as order of  $10^{-5}$  emu (that's why when normalizing, after dividing by a smaller volume (in the case of thin film), it brings up the magnitude of magnetization as seen in Fig. 11. It shows that most of the magnetic moments come from the surface and/or the interface between the film and the substrate, but not from the whole sample.

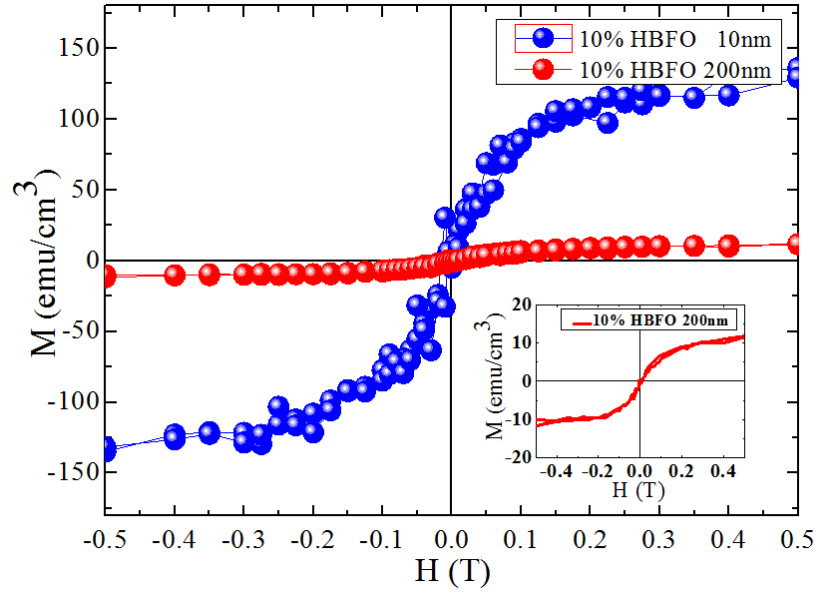


Fig. 11: Magnetization versus magnetic field taken at 300 K for  $\text{Ho}_{0.1}\text{Bi}_{0.9}\text{FeO}_3$  films with thickness of 10 and 200 nm. The inset shows the zoom for low field region of  $M$ - $H$  of the 200 nm-thick-film.

### 3.2.2. RE- doped BFO thin films

We can see that this is different from the Pr and Nd cases that even though magnetization is also large, but the structure of the very thin film seems to show some difference from the thicker one, not surface effect. This is similar to what we have observed in some other magnetic oxide systems [9]. This may be related closely to the tendency of defects and/or oxygen vacancies to locate more intensively at the surface and/or interface. This effect is more dominant in the Sm doping case (it can be seen while comparing Fig. 12 and Fig. 13. In the Ho case, even though there is also a strong surface/interface effect, magnetic moments still exist over the whole thickness of the film, however, with a much less density.

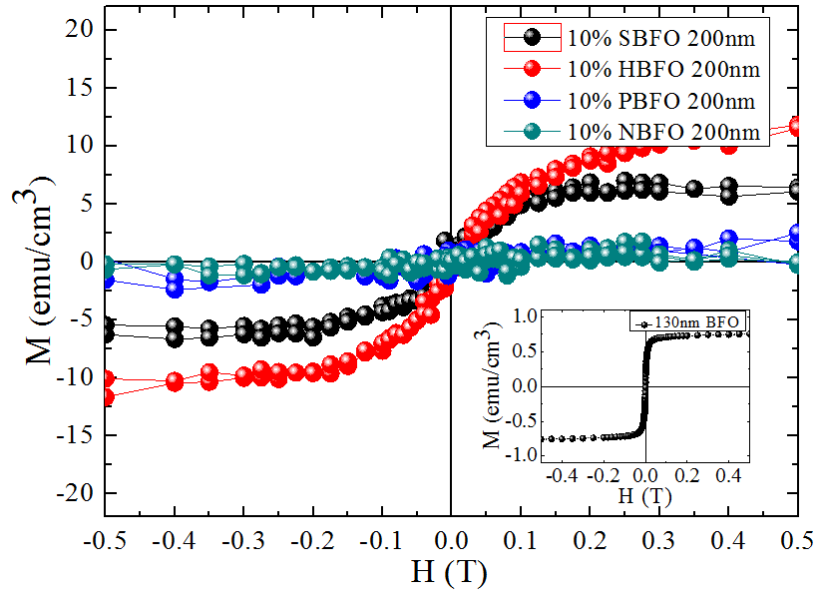


Fig. 12: Magnetization versus magnetic field taken at 300 K for 200 nm-thick  $\text{Re}_{0.1}\text{Bi}_{0.9}\text{FeO}_3$  films (where Re= Sm, Ho, Pr and Nd). The inset show the  $M$ - $H$  curves of undoped  $\text{BiFeO}_3$  films with similar thickness for comparison

Figs. 12 and 13 indeed give us a complete comparison for the magnetic properties of those four doping cases. As seen in Fig. 12, all of RE- doped BFO films (with the concentration of dopant of 10%) are ferromagnetic at room temperature. The  $M_s$  is quite large (the largest  $M_s$  is about  $11 \text{ emu/cm}^3$  for Ho doping case) and it is obtained at low field (0.2 T). RE- doped BFO films basically show a strong surface/interface effect: from Fig. 13, in comparison to Fig. 12, one can see that the thinner films have a much larger magnetization in comparison to the thick films. The largest obtained  $M_s$  is about  $1.5 \mu_B/\text{f.u}$  for the 10 nm-thick- Sm- doped BFO film. As for the case of Nd doping, even though the magnitude seen from Fig. 13 is not much different from that of Sm, the mechanism seems to be different.

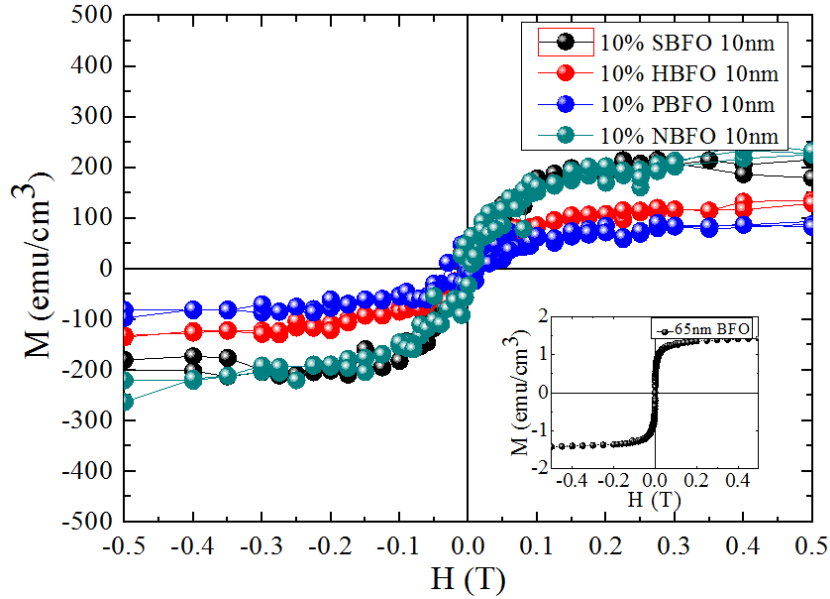


Fig. 13: Magnetization versus magnetic field taken at 300 K for 10 nm-thick  $\text{Re}_{0.1}\text{Bi}_{0.9}\text{FeO}_3$  films (where RE= Sm, Ho, Pr and Nd). The inset show the  $M$ - $H$  curves of undoped  $\text{BiFeO}_3$  films with similar thickness for comparison

Looking at the raw data of magnetic moment before normalizing, we find that the magnetic moment of the 10 nm-thick Nd- doped BFO film is one order larger than that of the 200 nm-thick-one. If the magnetic moments came basically from surface/interface, then those should have been maintained when the film is grown thicker, too (surface and interface exist in the thick film, and do not lose anywhere). From the XRD data that we analyzed earlier, no significant structural change is observed, except that the lattice parameter extended a bit more in the thinner films of Nd (and Pr). Somehow, the constrained is more relaxed in this case. What we should say here is that, for Sm- and Ho- doped BFO films, magnetism is mostly from the surface effect, but as for Pr and Nd case, nanostructure of the thin films with their confinement effects may play some important role. This may be also related to the big ionic radius of the latter case.

### 3.3. BFO Films' Chemical State

In order to identify the origin of magnetism of our RE- doped BFO thin films, XPS measurements were performed for the films with 10% of doping and thickness of 200 nm. A scan of the Fe 2*p* line is shown in Fig. 14. The peak of Fe 2*p* is expected at 711 eV for Fe<sup>3+</sup> and 709.5 eV for Fe<sup>2+</sup>. 10 Actually XPS is mostly sensitive to the surface of the films, so that to evaluate the ratio of Fe<sup>2+</sup>: Fe<sup>3+</sup> qualitatively would not be very correct. However, from the shape of the peaks one can say definitively that both Fe<sup>2+</sup> and Fe<sup>3+</sup> exist in all doping cases (Ho, Sm, Pr and Nd). The rough fitting analysis of the peaks give us the picture that the oxidation state of Fe in our films shows a coexistence of Fe<sup>2+</sup> and Fe<sup>3+</sup> with ratio is about 50% : 50% for the cases of Ho and Sm, and about 40% : 60% for the Pr and Nd cases. This is in accord with what was reported for BFO films made by sol-gel method [11]. The coexistence of Fe<sup>2+</sup> and Fe<sup>3+</sup> is in favor of the ferromagnetic phase in BFO films due to the double exchange between Fe<sup>2+</sup> and Fe<sup>3+</sup> via the role of oxygen as intermediates [11, 12]. When the amount of Fe<sup>3+</sup> is more favored, the ferromagnetism get weaker due to the fact the Fe<sup>3+</sup> - Fe<sup>3+</sup> interaction is in favor of antiferromagnetic ordering [12]. This explains why from the corresponding SQUID data shown in Fig. 12, we see that the magnetization of Pr and Nd- doped BFO films are much smaller than those of Sm and Ho- doped BFO films.

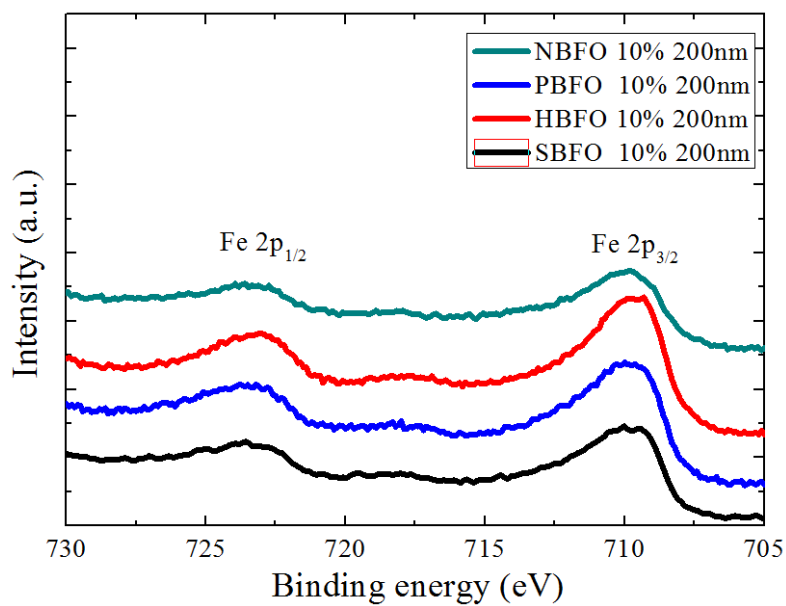


Fig. 14: XPS spectra of the Fe ions for the 200 nm-thick  $\text{Re}_{0.1}\text{Bi}_{0.9}\text{FeO}_3$  films (where RE= Sm, Ho, Pr and Nd)



## Chapter 4: Conclusions

Rare- Earth-(RE) doped BiFeO<sub>3</sub> thin films were grown on LaAlO<sub>3</sub> substrates using pulsed laser deposition technique. All the films show a single phase of rhombohedral structure with space group  $R\bar{3}c$ , and are room temperature ferromagnetic. Magnetic properties were found to be thickness dependent. The saturated magnetization in Ho- and Sm- doped films is much greater than those reported previously, and is observed at a much lower field as of 0.2 T. The magnetic moments of Ho- doped BFO and Sm- doped BFO films are roughly largest. The magnetization increases as the thickness decreases, suggesting that the observed behavior in Ho- and Sm- doped is indeed surface magnetism. The large magnetic moment was also obtained in very thin films of Nd- doped BFO, however, our data suggests another mechanism for this case. The observed ferromagnetism in our RE-doped BFO films should be caused by the coexistence of Fe<sup>2+</sup> and Fe<sup>3+</sup> that favor double exchange via oxygen.

## **Appendix**

- I.* The poster I presented in ICM 2012 Busan

# Effects of dimensionality on magnetization of Ho and Sm-doped BiFeO<sub>3</sub> Thin Films

T. Y. G. Kim<sup>1,\*</sup>, A.T. Raghavender<sup>1</sup>, S. Takashi<sup>2</sup>, and M. Kurisu<sup>2</sup>, Nguyen Hoa Hong<sup>1</sup>

<sup>1</sup>Nanomagnetism Lab, Department of Physics & Astronomy, Seoul National Univ., Seoul 151-747, Korea

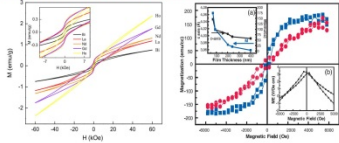
<sup>2</sup>Department of Physics, Graduate School of Science & Engineering, Ehime Univ., Matsuyama, Japan

\*tykim0922@gmail.com

## Motivation

### Surface magnetism in Rare-Earth (RE)-doped BiFeO<sub>3</sub> (BFO) thin films

Reports of other groups have suggested that by reducing the dimensionality, the spiral magnetic ordering could be suppressed. Thus multiferroics in thin films and nanocrystalline forms could enhance the magnetic properties. In BiFeO<sub>3</sub>, if Bi is substituted by a small amount of divalent or trivalent metal ions, or Fe is substituted by transition metal ions, a significant enhancement in magnetization can be achieved.

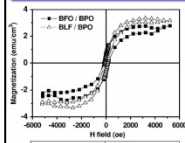


M vs H taken at Room Temperature (RT) for BFO (Re=La, Nd, Gd, and Ho) powders. Inset: enlarged curves showing the changes in the coercivity. P. Thakura J. Appl. Phys. 97 162504 (2010)

M vs H taken at RT for BFO 70nm thin film in & out of plane. Inset (a) is the thickness dependence of saturation magnetization (M<sub>s</sub>), (b) is preliminary ME measurement. J. Wang et al., Science 299 1717 (2003)

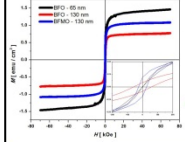
Therefore, we want to know the magnetization of RE-doped BFO thin films depending on the doping elements and thickness

## Previous studies



### RE doping effect

M vs H taken at RT for La-doped BFO films (H//). Doped one has a higher magnetization. Yi-Hsien Lee, Appl. Phys. Lett. 88, 042903 (2006)



### Thickness dependence

M vs H taken at RT for BFO thin films grown on LAO substrates. The thinner one has a higher magnetization. A.T. Raghavender, Mater. Lett. 55, 2788-2798 (2011)

## Fabrication

### Powder fabrication

- Starting powder made by Sol-gel method
- After grinding, it was annealed for 10 hrs @ 500 °C
- After grinding, it was annealed again for 10 hrs @ 900 °C.

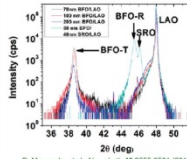
### Pulsed Laser Deposition (PLD) for thin film fabrication

PLD conditions	
Type	KF Excimer Laser (248 nm)
Target	R <sub>x</sub> Bi <sub>1-x</sub> FeO <sub>3</sub> ceramic target (x= 0.05, 0.1, Re= Sm, Ho)
Substrate	LaAlO <sub>3</sub> (5×5×0.5 mm <sup>2</sup> )
Substrate temperature	700 °C
Oxygen Partial Pressure	1.4×10 <sup>-4</sup> Torr
Repetition Rate	13 Hz
Energy density	210 mJ/cm <sup>2</sup>

During deposition, P<sub>O<sub>2</sub></sub> was kept as 1.4×10<sup>-4</sup> Torr, and after deposition, films were cooled down to 500K under the same P<sub>O<sub>2</sub></sub> as during deposition, with a rate of 20 °C/min.

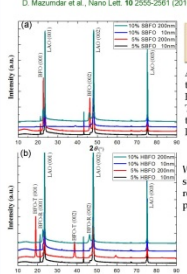
## Structural Analysis

### XRD analysis



Depending on thickness, concentration and dopants, the phase of RE doped BFO thin films can be changed.

There are two phases: Rhombohedral & Tetragonal.



### XRD patterns for (a) Sm-doped BFO thin films & (b) Ho-doped BFO thin films

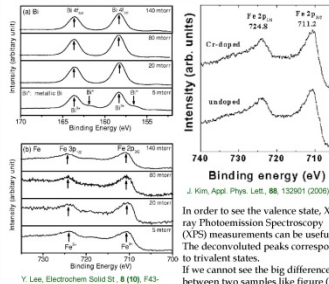
Among 8 thin RE-doped BFO thin films, only one, 5%, 200nm Ho-doped BFO, shows the Tetragonal phase. Every other thin films shows the Rhombohedral phase.

We need to do some calculations & simulations to understand the reasons of that single Rhombohedral phase.

XRD spectra show the well oriented samples, Both Rhombohedral and Tetragonal

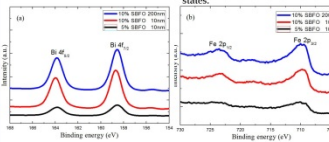
## Surface characteristics

### X-ray Photoelectron Spectroscopy (XPS) analysis



In order to see the valence state, X-ray Photoemission Spectroscopy (XPS) measurements can be useful. The deconvoluted peaks correspond to trivalent states.

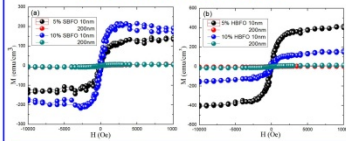
If we cannot see the big difference between two samples like figure (a), there is no big difference in valence states.



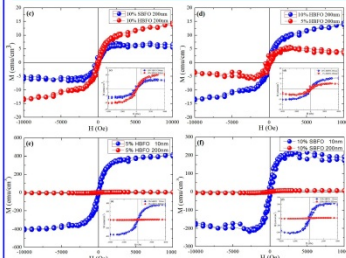
XPS spectra → Fe & Bi valence states are very small

## Magnetic properties

### Element & Thickness dependence



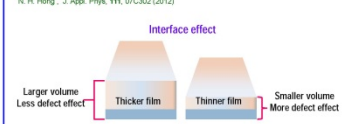
(a), (b) MH curves for films with different concentration, dopant and thickness.



From these figure, we can see the 2 crucial factors to induced magnetization; Thickness & Doped Element.

### Thickness dependence (Interface effect)

The thinner films can have as almost 100 times larger magnetic moment than other films. This suggests that if defects play a role for induced magnetization, then the interface and /or surface is the main origin.



## Summary

- The most dominant effect comes from thickness: Big magnetization comes from either Interface or Surface.
- Ho-doped BFO films seems to be advantageous than Sm-doped ones enhancing magnetization.
- Magnetization of RE-doped BFO thin films are type of dopant, concentration of dopant and thickness dependent.

## References

- [1] P. Thakuria and P.A. Joy, Appl. Phys. Lett. **97**, 162504 (2010).
- [2] J. Wang J. B. Neaton, H. Zheng, V. Nagarajan, S. B. Ogale, B. Liu, D. Viehland, V. Vaithyanathan, D. G. Schlom, U. V. Waghmare, N. A. Spaldin, K. M. Rabe, M. Wuttig, R. Ramesh , Science **299**, 1719 (2003).
- [3] N. H. Hong, J. Sakai, N. Poirot, and V. Brizé, Phys. Rev. B **73**, 132404 (2006).
- [4] J. Liu, L. Fang, F. Zheng, S. Ju, and M. Shen, Appl. Phys. Lett. **95**, 022511 (2009).
- [5] F. Z. Quian, J. S. Jiang, S. Z. Guo, D. M. Jiang, and W. G. Zhang, J. Appl. Phys. **106**, 084312 (2009).
- [6] Lange's Handbook of Chemistry" 16th Edition, Edited by James G. Speight, McGraw-Hill publisher (2005).
- [7] D. S. Rana, K. Takahashi, K.R. Mavani, I. Kawayama, H. Murakami, and M. Tonouchi, Phys. Rev. B **75**, 60405 (2007).
- [8] A. T. Raghavender, N. H. Hong, C.-K. Park, M.-H. Jung, K.-J. Lee, and D.-S. Lee, Mat. Lett. **65**, 2786 (2011).
- [9] N. H. Hong, J. Sakai, and F. Gervais, J. Mag. Mater. **316**, 214 (2007).
- [10] T. Schedel-Niedrig, W. Weiss, and R. Schlögl, Phys. Rev. B **52**, 17449 (1995).
- [11] Y. Wang, Q. H. Jang, H. C. He, and C. W. Nan, Appl. Phys. Lett. **88**, 142503 (2006).
- [12] P. R. Lear, and J. Stucki, Clays and Clay Minerals **35**, 373 (1987).
- [13] J.H. Song,(2012), 'Ferromagnetism in C-doped SnO<sub>2</sub> thin films', Seoul National University, Master thesis
- [14] [http://pruffle.mit.edu/atomiccontrol/education/xray/xray\\_diff.php](http://pruffle.mit.edu/atomiccontrol/education/xray/xray_diff.php)
- [15] <http://www.csiro.au/en/Organisation-Structure/Divisions/Earth-Science--Resource-Engineering/geophysics/Superconducting-quantum-interference-devices.aspx>
- [16] [http://www.vub.ac.be/META/toestellen\\_xps.php?m=xpand&d=menu7](http://www.vub.ac.be/META/toestellen_xps.php?m=xpand&d=menu7)

## 국문초록

### 상온의 낮은 자기장에서 높은 자기 모멘트를 보이는 희토류가 첨가된 비스무스 철산화물의 강자성

비스무스 철산화물( $\text{BiFeO}_3$ ; BFO)은 높은 강유전 상전이 온도(1103 K)와 높은 반강자성 상전이 온도(640 K)를 가지고 있는 축방받는 다중강성 물질이다. 이전의 연구결과에 따르면, 차원을 줄이면서 나선형 자성적 질서가 억제되어 자성적 특성이 달라질 수 있다. BFO에서 비스무스(Bi)는 소량의 2가나 3가 금속이온들로, 철(Fe)은 전이금속으로 치환되어 자성이 눈에 띄게 증가된다. 희토 금속(Sm, Ho, Pr, Nd)이 도핑된 BFO 박막을 펄스레이저 증착법(PLD)을 이용해서  $\text{LaAlO}_3$  기판위에 증착시켰다. 모든 박막은 단상(single phase)이고, 공간군(Space group)이  $R3c$ 인 롬보헤드랄 구조를 보인다. 홀뮴(Ho)과 사마륨(Sm)이 첨가된 박막에서는 0.2 테슬라의 작은 자기장에서도 이전 연구보다 강화된 포화 자성이 측정됐다. 이 경우는 박막의 두께가 얇아질 수록 자성이 증가됐고, 이는 표면효과(surface effect)로 인한 현상으로 예상된다. 네오디뮴(Nd)이 첨가된 경우는 얇은 박막이 더 큰 자성 모멘트를 가지지만, 그 원리가 다른 것으로 보인다.

주요어: 비스무스 철산화물, 희토류, 상자성, 박막

학번: 2011-20396